The Spiral Host Galaxy of the Double Radio Source 0313-192 [1]

William C. Keel

Department of Physics and Astronomy, University of Alabama, Box 870324, Tuscaloosa, AL 35487; keel@bildad.astr.ua.edu

Raymond E. White III

Department of Physics and Astronomy, University of Alabama, Box 870324, Tuscaloosa, AL 35487; rwhite@bama.ua.edu

Frazer N. Owen

National Radio Astronomy Observatory[2], P. O. Box O, Socorro, NM 87801.

Michael J. Ledlow[3]

Gemini Observatory, Southern Operations Center, AURA, Inc., Casilla 603, La Serena, Chile.

ABSTRACT

We present new *Hubble*, *Gemini-S*, and *Chandra* observations of the radio galaxy 0313-192, which hosts a 350-kpc double source and jets, even though previous data have suggested that it is a spiral galaxy. We measure the bulge scale and luminosity, radial and vertical profiles of disk starlight, and consider the distributions of H II regions and absorbing dust. In each case, the HST data confirm its classification as an edge-on spiral galaxy, the only such system known to produce such an extended radio source of this kind. The *Gemini* near-IR images and *Chandra* spectral fit reveal a strongly obscured central AGN, seen through the entire ISM path length of the disk and showing X-ray evidence of additional absorption from warm or dense material close to the central object. We consider several possible mechanisms for producing such a rare combination of AGN and host properties, some combination of which may be at work. These include an unusually luminous bulge (suggesting a black hole of mass $5-9\times10^8$ $M_\odot$), orientation of the jets near the pole of the gas-rich disk, and some evidence of a weak gravitational interaction which has warped the disk and could have enhanced fuelling of the central engine. We detect an X-ray counterpart of the kiloparsec-scale radio jet emerging to the south; jet/counterjet limits on both radio and X-ray regimes allow them to be symmetric if seen more than 15° from

the plane of the sky, still consistent with the jet axes being within $\sim 30^\circ$ of the poles of the gas-rich galaxy disk. A linear or disklike emission-line structure is seen around the nucleus, inclined by $\sim 20^\circ$ to the stellar disk but nearly perpendicular to the jets; this may represent the aftermath of a galaxy encounter, in which gas is photoionized by a direct view of the nuclear continuum.

Subject headings: galaxies: spiral – galaxies: active — galaxies: individual (0313-192)

1. Introduction

The relationships between active galactic nuclei (AGN) and their host galaxies may be important not only for the evolution of the AGN, but for the host galaxies themselves. Since dynamical evidence supports the existence of massive black holes in numerous galactic nuclei, and very general arguments suggest that the active growth of such black holes by accretion is what we see as AGN, the current demographics of such black holes must result from the whole history of AGN episodes. Furthermore, some aspects of galaxy formation become easier to understand if AGN episodes regulate the properties of gas in galaxies via such feedback mechanisms as heating or wind sweeping. These factors have renewed interest in the connections between properties of AGN and their host systems.

Among the most durable systematic patterns between the occurrence of AGN and the structure of surrounding galaxies has been the finding that large double radio sources occur only around elliptical galaxies, or systems that plausibly would have been called ellipticals until a recent external disturbance (in studies ranging from Matthews, Morgan, & Schmidt

---

[1]Based on observations made with the NASA-ESA *Hubble Space Telescope* obtained at the Space Telescope Science Institute, which is operated by the Association of Universities for Research in Astronomy, Inc., under NASA contract No. NAS5-26555; with the *Chandra* X-Ray Observatory; and on observations obtained at the Gemini Observatory, which is operated by the Association of Universities for Research in Astronomy, Inc., under a cooperative agreement with the NSF on behalf of the Gemini partnership: the National Science Foundation (United States), the Particle Physics and Astronomy Research Council (United Kingdom), the National Research Council (Canada), CONICYT (Chile), the Australian Research Council (Australia), CNPq (Brazil), and CONICET (Argentina)

[2]The National Radio Astronomy Observatory is a facility of the National Science Foundation, operated under cooperative agreement by Associated Universities, Inc.

[3]Deceased 2004 June 5.

1964 to Heckman et al. 1986). This correlation has figured in theoretical explanations of large-scale jets, and in understanding why such jets are associated with extensive synchrotron lobes. There are a handful of nearby radio galaxies showing evidence for gas-rich disks, generally in host galaxies so disturbed that these are well explained as captured material from major mergers – 3C 120 (Arp 1975; Heckman & Balick 1979; García-Lorenzo et al. 2005), 3C 293 (van Bregel et al. 1984; Floyd et al. 2006), 3C 305 (Heckman et al. 1982; Jackson et al. 2003), and 3C 285 (Roche & Eales 2000) are well-studied examples. In each of these, the system is disturbed enough to leave its original galaxy type ambiguous. While *normal* spiral galaxies with AGN often have kiloparsec-scale radio jets; no previously reported case of a large-scale double radio source associated with a spiral has withstood detailed examination as regards both the host Hubble type and its identification with the radio source. In contrast, the edge-on galaxy associated with the radio source 0313-192 in the cluster Abell 428 obviously has a significant stellar disk (Ledlow, Owen, & Keel 1998), and a prominent dust lane of the kind usually associated with spiral galaxies. We report here *Hubble* ACS, *Gemini-S*, and *Chandra* ACIS images of this galaxy, resulting in quantitative photometric evidence that the galaxy is in fact a spiral, and pointing to peculiar features of its gas distribution which may shed light on how this rare combination of galaxy and nuclear activity happened.

As shown by Ledlow et al. (2001), the radio structure of 0313-192 includes a nuclear source, a nuclear jet toward the southern lobe of about the same extent as that in M87 but several times less powerful, larger twin jets directed at projected angles of about 70° to the galaxy disk plane, and edge-darkened lobes spanning roughly 280″ (about 360 kpc at $z = 0.067$ for H_0=70 km s^{-1} Mpc^{-1}). This structure would typically fall into Fanaroff-Riley type I (FR I), a classification in which it would lie near the middle of the power distribution ($\approx 10^{24}$ W Hz^{-1} at 1400 MHz). Strong 21-cm H I absorption is detected against the central source at a column density $N_H > 10^{22}$ cm^{-2}, with the limit set by its large optical depth and the resolution of the data (Ledlow et al. 2001). The H I absorption is also narrow in velocity span (34 km s^{-1} FWHM), more characteristic of a line of sight cutting radially through a large disk than one dominated by gas closer to the central mass. This large column density is comparable to what we see toward Sgr A, supporting the idea that we are seeing a galaxy similar to our own viewed exactly edge-on.

2. Observations

2.1. HST ACS imaging

Images in broad and narrow bands were obtained with the Advanced Camera for Surveys (ACS) on board HST, on 16 July 2002, using the Wide-Field Camera (WFC). Two broad bands, F555W (V) and F775W (I), were observed for total exposures of 1100 seconds each, split for cosmic-ray rejection. The redshifted wavelengths of [O III] and Hα+[N II] were observed using the ACS linear ramp filters (LRF) for 2500 seconds each, again split for cosmic-ray rejection. For [O III] the FR551N ramp filter was centered at 5342 Å, while Hα+[N II] were observed with ramp FR716N set to 7003 Å. Since wavelengths are set by rotating the filters in ACS, positioning of the target was consistent between these two narrow-band images, requiring only a single set of offsets between continuum and narrow-band images for registration and continuum subtraction. These filters have nominal half-power bandwidths of $\Delta\lambda/\lambda = 0.02$. Thus, the [O III] setting excludes the λ4959 line, while the Hα image includes the adjacent [N II] lines.

To verify the registration of the optical and radio coordinate systems, we used 11 stars and compact galaxies listed in the USNO A-2 astrometric catalog lying within the ACS field on the broadband images. The coordinate offsets derived from individual stars have scatter $\sigma = 0.1$ arcsecond (2 ACS WFC pixels), so we consider that coordinates derived from the HST frames using this correction are on the VLA reference frame to roughly this accuracy. The overall correction from header to astrometric coordinates using these reference stars is -0.1016 seconds in RA and -1.26″ in declination.

Based on this registration, the radio core coincides closely with the galaxy nucleus, as measured from the center of the I-band bulge isophotes. The radio core (α =03:15:52.10, δ =-19:06:44.4 in the J2000 frame) is within 0.20" of the bulge center, as derived from ellipses fit to large arcs of the isophotes at a semimajor axis of 1". Such a tight match (within 2σ) gives us confidence that the radio source and galaxy are indeed the same object. For visual reference, Fig. 1 shows a composite VLA A-array image, where the outer regions are as seen at 1.4 Ghz and the inner jet is from an 8.5-Ghz observation, superimposed on the color rendition of the ACS imagery. The prominent grand-design spiral to the northwest is not a good candidate for a physical companion, lying at $cz = 15225 \pm 87$ km s^{-1} (Ledlow et al. 2001), as opposed to a redshift of $cz = 20143 \pm 66$ for 0313-192 itself. A combination of sparse galaxy population and large redshift spread led Ledlow et al. to suggest that Abell 428 is more like a filament seen end-on, rich in small groups, than a cluster environment.

Fig. 2 shows the smaller-field view in the continuum, as a composite color display. This view emphasizes the intricate structure in the disk dust lane, and the blue star-forming

regions seen around the disk warp.

Continuum-subtracted emission-line images were constructed using the broadband images as continuum, with the correction for line radiation in these bands being small. The relative shifts between broad- and narrow-band images could be checked from the data themselves only to the ±2 pixel level, since there are no bright unresolved sources in the region of useful LRF transmission, but this should cause no particular problem in the analysis since we see no features with the positive/negative pattern which would result from subtraction of an inappropriately shifted continuum. The scaling factors to account for the continuum included in the narrow bands were empirically determined from field stars and the galaxy bulge. For Hα, since the line wavelength is near the blue edge of the F775W passband, an improved continuum subtraction was possible using an interpolated 7000-Å image obtained as a weighted average of the V and I images. The emission-line images are shown in Fig. 3. The color of reddened light in the dust lane is extreme enough that we cannot simultaneously get a proper continuum subtraction there and in the rest of the galaxy; some negative residuals appear in the dustiest areas.

In a search for UV continuum emission from the inner knots in the radio jet on the SW side of the nucleus, we also obtained a UV continuum image using the ACS High-Resolution Camera (HRC) and F250W filter, in a 2600-second exposure pair. A few faint sources are detected near the galaxy but none coincident with either disk star-forming regions or jet knots. This stands in contrast to our soft X-ray detection of the southern jet out to about 3″ from the core (section 5). Our detection limit for compact sources allows a single power-law specrtum between radio and X-ray measurements.

2.2. Gemini-S NIR imaging

Images of 0313-192 in the J,H, and K_s bands were obtained using the FLAMINGOS system at the 8-m *Gemini-South* telescope, during a commissioning run on 13 October 2001. For each, a set of 100-second exposures in a 3×3-pointing offset pattern was combined, with offset sky measurements interspersed. The mean delivered image quality (DIQ) was 0.39" FWHM, sampled with 0.078" pixels. The images are compared in Fig. 4. Their resolution is sufficient to reveal the dust lane clearly at J and H, while a central source is progressively more prominent at H and K. This light comes from some combination of the inner starlight, increasingly visible through the dust lane, and the AGN itself, possibly even more heavily reddened.

We used the Apache Point data from Ledlow et al. (1998) to set the photometric scale

for the FLAMINGOS images. The central region, within the seeing disk, has $J - K = 1.6$, compared to the surrounding bulge light at $J - K \approx 1.0$. The spatial distribution of the redder component is consistent with a contribution from a central point source. This, coupled with the K magnitude of the central source, suggests that we are seeing the central AGN in addition to reddened light from the obscured part of the bulge (section 4).

2.3. Chandra ACIS observations

A 19.2-ksec observation of 0313-192 (ObsID number 4874) was obtained in February 2004, with the galaxy located at the ACIS-S aimpoint. This was done for best sensitivity at lower energies, since the active nucleus was likely to be deeply obscured by foreground gas. This proved to be the case, with strong low-energy absorption. As discussed in section 4, the best fit for an absorbed power-law spectrum has a large column density $N_{\rm H} = 4.06^{+0.73}_{-0.58} \times 10^{22}$ cm^{-2} and a hard photon index $\Gamma = 1.33^{+0.34}_{-0.27}$.

The strong absorption against the nucleus allows a sensitive search for surrounding structures at low energy. As discussed in section 5, this approach allows us to detect emission below about 3 keV from the southern jet previously mapped at 3.6 cm by Ledlow et al. (2001).

3. Morphology of 0313-192

The key question we address with the new optical and near-IR data is the morphological type of this galaxy — is there unequivocal evidence that it is a spiral? The ACS images show the classic appearance of an edge-on disk galaxy (Fig. 2). Both the dust lane and stellar disk indicate that we view this galaxy within 0.5° of edge-on, so morphological classification must rely on secondary characteristics rather than on the properties of the spiral arms. These images are of high enough resolution that we can compare 0313-192 in some detail to local galaxies which are agreed to be edge-on spirals of well-constrained Hubble type.

3.1. Bulge

The ACS data allow a much better view of the bulge than previous images, so we can fit regions free of significant obscuration to derive unambiguous luminosity and scale values. The bulge isophotes, traced in regions where dust is not a problem, remain slightly boxy, which limits the precision with which we can fit a bulge model. We fitted a variety of de

Vaucouleurs ($r^{1/4}$) profiles to the bulge, varying the effective radius and axial ratio, and assessed the goodness of fit by RMS residuals in several apparently dust-free bulge regions, after subtracting an approximate disk model. Our best bulge fit to the I-band image has axial ratio $b/a = 0.6$ and effective radius 50 pixels (2.5″), which is likely determined at the 10% level. Normalizing to fit the brightest bulge regions gives this fit a total brightness corresponding to Cousins $I = 15.08$, taking the magnitude transformations from the STMAG system definition and Fukugita et al. (1995). This translates to a very luminous bulge, brighter than our earlier estimates (Ledlow et al. 1998) mostly because a significant fraction of the bulge luminosity is obscured by the dust lane. The bulge luminosity will be used in section 4 to consider the expected mass of a central black hole.

3.2. Stellar disk

Surface photometry of edge-on spirals has been used extensively to study the vertical structure and dynamics of disk stars, providing a large body of comparison data. As found originally by van der Kruit & Searle (1981), the starlight distribution parallel to the disk plane in edge-on spirals, after bulge subtraction, is well expressed by the projection of a radially truncated exponential disk, with this truncation occurring at radii of several exponential scale lengths. Similar behavior is found in 0313-192 (Fig 5). After subtracting our bulge model, we find a good fit for radial scale length of 109 pixels (5.4″, 6.9 kpc) truncated at 20.8 kpc (3.0 scale lengths, which projects to 16.2″). This applies for a range of height north and south of the disk plane, once we adjust the assumed position angle of the disk for best symmetry on east and west sides (determining this orientation at the 0.1° level). The limit in measuring the orientation and scale length is set by small asymmetries in the disk which persist on both north and south sides and in both passbands.

Similarly, the profile of edge-on spiral disks perpendicular to the disk plane is well described by a single exponential, nearly independent of radius (van der Kruit & Searle 1981; de Grijs, Peletier, & van der Kruit 1997). This also applies to 0313-192 (Fig. 5). Studies of edge-on galaxies with a range of morphological type have shown that the ratio of disk scale length to vertical scale height varies systematically with stage along the Hubble sequence, in the sense that the disk is typically thinner relative to its radial scale length for later Hubble types (Schwarzkopf & Dettmar 1997). Using the data from Pohlen et al. (2000), who tabulate scale heights which are twice the scale height fitted for an exponential, disks as thin as we find in 0313-192 are found only for spirals of type Sb (de Vaucouleurs T type 3) and later (the S0 distribution includes only a few which are nearly this thin). This is further evidence that, were 0313-192 to be viewed more face-on, it would appear as a clear spiral.

Note, in this context, that some analyses use either a theoretically motivated $\mathrm{sech}^2(z)$ form or a compromise sech (z) law in fitting the vertical disk profile; the available observations do not clearly support one of these as superior to the empirical (albeit theoretically problematic) exponential version.

The $V-I$ colors of the bulge and most of the disk are quite similar. This fact, and the scale height of the disk in 0313-192, suggest that much of what we see is a "thick disk". However, the blue star-forming layer in the midplane can be seen where the warp allows us to see around the dust lane, and its intensity profile forms a virtually continuous exponential with the starlight farther from the plane. Thus, the parts of the disk we can see may form a useful basis for estimating the bulge:disk flux ratio, interpolating across obscured regions with the combination of de Vaucouleurs bulge model and double-exponential disk. Our best-fit parameters yield an I-band bulge:disk ratio of 0.4; this would be slightly smaller in the V band because the midplane star-forming regions become more important. Again, from our vantage point, both components suffer strong optical obscuration, so this estimate of a dust-free value differs from our initial estimates made directly from lower-resolution images. Even neglecting hidden star-forming regions, our photometric model makes 0313-192 a very luminous spiral; only 10 spirals of the 895 in the Revised Shapley-Ames Catalog (Sandage & Tammann 1981) would outshine it, and such an apparent-magnitude-limited sample is already biased on favor of luminous galaxies.

3.3. Star-forming regions

The [O III] and Hα+[N II] images (Fig. 3) show discrete objects in the disk plane which are bluer than their surroundings in $V-I$. These are normal H II regions, as shown by the emission-line ratios spatially integrated over large regions of the disk (Ledlow et al. 1998) We see these at optical wavelengths only thanks to the warped disk plane, which allows large windows where our view penetrates close to the midplane.

The only ambiguity in the galaxy classification is whether 0313-192 could possibly be an S0. When S0s host significant star formation, as traced via Hα imaging, its distribution is sharply confined on the outer edge, in an annulus with or without a filled center of star formation (Pogge & Eskridge 1993, Macchetto et al. 1996, Koopmann & Kenney 2006). This distribution follows the locations of their dust lanes. In 0313-192, star-forming regions seen around the dusk warp extend as far as the dust, and both extend as far as $13''$ (17 kpc) from the nucleus. The stellar disk can be traced only slightly farther, to about 21 kpc.

3.4. Dust lane

The dust lane shows a distinct warp, by about 3° in projection with respect to the midplane of the stellar disk. This appearance could result even if both share an identical warp, because of the weighting of dust visibility to the front side of the disk while the starlight as seen around the dust is closer to the line-of-sight integral of its distribution.

The dust lane in 0313-192 is thick, exhibits rich vertical structure, and spans virtually the entire radial extent of the stellar disk. All these features are characteristic of spirals with active disk star formation, rather than of S0 galaxies which may also have dust in the disk plane. As shown in detail in Fig. 6, the thick opaque dust lane is accompanied by localized features extending to 0.8 kpc from the plane. These are often seen in nearby edge-on spirals, with some evidence that their occurrence and extent correlate with the disk star-formation rate (Howk & Savage 1999). Such lanes are generally much thinner in edgewise S0 systems, although recent Hubble Heritage imaging of NGC 5866 shows that even these galaxies can show a detectable level of vertical stirring in their dust lanes.

As noted above, the dust lane is detected to a radial distance of 12.5″ from the nucleus (projecting to 16 kpc), nearly the same extent over which the stellar disk is found. This also argues for a genuinely spiral nature, since S0 galaxies with dust lanes show them over only a fraction of this radial extent. In every instance of edge-on S0 systems shown in the Carnegie Atlas (Sandage & Bedke 1994), and as discussed in their text accompanying images of dusty S0 galaxies, the dust is in an annular distribution truncated well within the visible stellar disk, which is not necessarily the case in spirals. This is true for S0 galaxies classified not only in the revised Hubble system developed by Sandage, but with the slightly different criteria used in the de Vaucouleurs system (Buta, Corwin, & Odewahn 2006). In both classification systems, edge-on spirals have dust distributions which are less confined radially, and can have the same scale length and detected extent as the stellar disk. Thus, the dust structure in 0313-192 is most clearly characteristic of a spiral galaxy rather than even a relatively dust-rich S0 system. We illustrate this through a comparison (Fig. 6) of 0313-192 with several nearby galaxies having widely-agreed-upon Hubble types. These local examples are all bright, with large angular size, and have concordant Hubble types in both the Sandage and de Vaucouleurs extensions of the Hubble system (using types taken from the Sandage & Tammann 1987, Sandage & Bedke 1994, and Buta et al. 2006). This comparison is in the spirit of the demonstration by Curtis (1918) that spirals seen at various angles form a continuous sequence, and that their disk planes are marked by optically thick absorbing regions. In fact, all of the nearby comparison galaxies we show were also included in Plate III of Curtis' discussion.

4. The nucleus

The reason for a spiral galaxy producing such a rare manifestation of nuclear activity as this double radio source might lie ultimately in unusual properties of the AGN itself. Previous data have illustrated the existence of a core radio source and emission-line gas characteristic of type 2 Seyferts or narrow-line radio galaxies. Our new data allow us to probe additional properties of the nucleus in several ways.

4.1. A tilted circumnuclear emission-line structure

The emission-line images (Fig. 3) show a roughly linear structure inclined by about 20° to the disk plane. This structure has a higher excitation level than the emission-line gas seen elsewhere in 0313-192. Using the nominal filter throughput values from the ACS online exposure calculator, the disk H II regions have [O III] λ5007/(Hα+[N II] ratios in the range 0.39-0.48, typical of H II regions in luminous spirals with metal-rich disk gas. The anomalous tilted emission regions have consistent values on both sides of the dust lane, [O III] λ5007/(Hα+[N II] = 1.00 ± 0.03. A slightly lower value (0.85) is seen for gas near the nucleus north of the dust lane away from the tilted structure, and the prominent single knot southeast of the nucleus has a level (1.02) consistent with the anomalous feature. This emission must have been mostly responsible for the Sy 2-like spectroscopic signature found by Ledlow et al. (1998). The only significant ionization structure within this feature is that the [O III] emission is relatively weaker near the edge of the dust lane, which can be plausibly attributed to extinction.

These data give us very limited information on the nature of this structure, and even whether it might be part of an inclined disk of gas or more akin to an ionization cone. The latter seems unlikely because it makes a large angle with the inner radio jet axis ($\approx 80°$ in projection), and the radio jet falls outside the projection of the putative ionization cone. An inclined gaseous disk would fit with the warped stellar disk as evidence of a minor merger or more distant encounter, perhaps several disk-crossing times before our current view. In this view, this gas, and a single knot (to the upper right of the nucleus in Fig. 3) some distance from the main gaseous disk, must be ionized by a direct view of the central AGN, to account for their similar excitation levels.

If it is part of a ring or inclined disk, it is noteworthy that this gas distribution is within 10° in projection of being perpendicular to the radio axis, which would make sense if the central black hole were accreting material with this same overall direction of angular momentum. Since we see warps in two scales – the warped dust disk (which may itself

sample a warp which exists in the stellar disk, but is less apparent due to the different weighting of starlight along the line of sight), and the inclined potential inner gas-rich disk – both might be attributed to a minor merger or other gravitational disturbance. While minor warping can in principle be excited by internal mechanisms (Bertin & Mark 1980), the 20° tilt of the emission-line feature seems to require an externally forced origin. Such a disturbance might increase the accretion rate of the central black hole and be a factor in producing this unique manifestation of activity from a spiral galaxy. However, the timescales for differential precession should scale with orbital period, meaning that the inner structure should be more phase-wrapped and less well-defined than the outer warped structure (as in the evolution of an accreted polar ring as well as less dramatic tidally-induced warps; Hunter & Toomre 1969). In this light, producing both warps with a single event would require either that there are two narrow annuli, so that differential precession could leave each annulus relatively intact, or the two warps have different origins. For example, the dust warp might be due to tidal forces during an encounter from which the disturber was mostly accreted, with its gas forming the inner emission-line structure.

4.2. IR detection of a reddened AGN

The central very red structure in the *Gemini* images (section 2.2) is well explained by a reddened point source located behind the dust lane. However, it is not bright enough to absolutely require this to be an AGN rather than the reddened peak of the bulge starlight. We experimented with subtracted scaled versions of the best-fit de Vaucouleurs bulge (section 3.1) from the K_s image, and find that the central intensity always falls short of the unreddened inward extrapolation of the bulge light. A tighter constraint incorporates the $J-K$ color excess from the dust lane, which is just resolved in the *Gemini* images. Relative to the adjacent unobscured disk light, the dust lane is 0.7 magnitude redder in $J-K$. For a Galactic reddening law, $E(J-K) = 1.8A_K = 0.18A_V$. In this case, these values suggests that material directly behind a typical piece of the dust lane is obscured by only 1.3 magnitude at K. The central flux shortfall of the scaled bulge model (when matched to the outer bulge isophotes, yielding disk residual isophotes which are nearly straight across the bulge region) is almost exactly a factor 2, implying that the galaxy has a central flux excess of 64% of the central bulge luminosity (within a radius of $0.94''$), or roughly $K = 15.7$ after correcting for our mean extinction in the dust lane. Structure in the dust lane could change this limit; in particular, it is likely to be an underestimate given the nondetection of a central source in even the I ACS image. Taken as a lower limit, this implies that the AGN has $M_K < -21.5$. Typical QSOs are brighter than $M_K = -23.5$ (e.g., Percival et al. 2001).

4.3. Hard X-ray continuum

X-rays may give us the most direct view of the nucleus in this system, given the ambuguity in unravelling the radio contributions of the core and small-scale jet emission.

We used *XSPEC* to fit an absorbed power law to the *Chandra* spectrum, extracted within a 2″ radius. We adopted a fixed Galactic column of 3.1×10^{20} cm^{-2} (derived from the *HEASARC* nH tool) and included an intrinsic absorption component at the redshift of the galaxy. With a count rate of ~ 0.1 cnt s^{-1}, the source is mildly piled up, so we applied the *XSPEC* pileup model. The best fit (Fig. 7) has a χ^2 per degree of freedom $\chi^2_\nu = 1.11$, a photon index of $\Gamma = 1.33^{+0.34}_{-0.27}$ (90% confidence intervals) and an intrinsic absorbing column of $N_H = 4.06^{+0.73}_{-0.58} \times 10^{22}$ cm^{-2}. This absorption is broadly comparable to the 10^{23} cm^{-2} reported toward Sgr A itself (Baganoff et al. 2003), which make sense since both lines of sight pass through much of the disk plane of spiral galaxies. The unabsorbed flux for this model fit would be 3.34×10^{-12} erg s^{-1} cm^{-2} in the 0.5-4.5 keV band and 4.88×10^{-12} erg s^{-1} cm^{-2} in the 2-10 keV band. These translate into luminosities of $L_X = 3.6 \times 10^{43}$ erg s^{-1} (0.5-4.5 keV) and $L_X = 5.3 \times 10^{43}$ erg s^{-1} (2-10 keV). These luminosities are comfortably in the range occupied by both broad- and narrow-lined radio galaxies (e.g. Grandi et al. 2006) and only slightly less luminous than recent detections of type II QSOs (Ptak et al. 2006).

We considered a partial-covering fit to the X-ray data to (at least formally) improve the fit at the lowest energies. Including a variable covering factor does slightly improve the χ^2, by $\Delta\chi^2 = 6.6$ on adding one additional parameter (to $\chi^2 = 118$ for 111 degrees of freedom). The absorbing column density increases by 6% with respect to the range listed anove, for complete coverage, and the photon index steepens by 0.13 (both changes lying well within the confidence intervals). The fitted covering fraction is essentially unity, with the fit yielding a value of 0.995 but raising the implied column density by $\sim 20\%$.

As set out by Evans et al. (2006), there has been considerable discussion about whether the X-ray emission from radio-galaxy cores arises from the central engine itself or from a parsec-scale jet. Evans et al. consider the ranges of X-ray luminosity, absorbing column density, and spectral shape over a variety of bands to address the issue, noting that the mean X-ray properties are quite different between FR I and FR II sources. In their sample, FR I radio galaxies have modest absorption, with only one of 15 having $N_H > 10^{23}$ cm^{-2}, while all but one of the 7 FR II nuclei have column densities above this value. They attribute this to dense circumnuclear tori in FR II nuclei. In the case of 0313-192, the geometry of the host galaxy combined with the amount of foreground absorption mean that we must consider a substantial role for absorption in the host galaxy as well as around the nucleus.

The equivalent column density found from X-ray absorption is $N_H = 4 \times 10^{22}$ cm^{-2}

(above). This is significantly greater than the H I column density measured from 21 cm absorption ($N_H \approx 10^{22}$ cm^{-2}; Ledlow et al. 2001). The conversion from absorption profile to column density includes the H I spin temperature T_s and the ionized fraction of hydrogen, so that absorption by progressively warmer and more ionized gas leaves a smaller H I signature. This mismatch leads us to consider more complex models for the absorbing gas. Much of the H I is undoubtedly in normal cold clouds in the galaxy disk, but conditions near the AGN could differ in several ways. In dense regions, T_s approaches the kinetic temperature, decreasing the absorption per atom (for example, by a factor ≈ 4 at $T_s = 600$ K). Similarly, fully ionized absorbing gas appears only in the X-ray accounting. Just as X-ray absorption in excess of the foreground Galactic H I value is often considered to be intrinsic to active nuclei, we may here be dealing with absorption from warm or dense material close to the active nucleus accounting for more than half the X-ray value. Since we probably view the inner jets within 30° of the plane of the sky, any dense gaseous torus would be viewed within 30° of edge-on. Polar opening angles of these structures are typically no smaller than this, to account for the relative numbers of types 1 and 2 Seyfert galaxies and broad- and narrow-line radio galaxies as well as structures of ionization and scattering cones (e.g., Antonucci 1993, Clarke et al. 1998), so it is plausible that this excess absorption arises in such a structure very close to the central source. The circumnuclear absorption may be strong enough to require an unusually extensive or dense torus; both host-galaxy and derived circumnuclear absorption are an order of magnitude larger that in the Seyfert nucleus IC 4329A (Steenbrugge et al. 2005), whose host galaxy is viewed with similar geometry. Analogous evidence for warm or dense circumnuclear H I in Seyfert galaxies has been discussed by Gallimore et al. (1999), particularly with regard to suppression of H I absorption near the active nuclei. This warm or dense absorber might also contribute to the spectral turnover observed between 1.4 and 8.5 Ghz in the core of 0313-192 (Ledlow et al. 2001), through free-free absorption, although the density dependence of the emission measure needed to calculate its strength makes comparison with column densities difficult.

4.4. Bulge properties and the expected black-hole mass

The bulge luminosity-black hole mass relation, while showing much more scatter than the relation between central mass and stellar velocity dispersion, can offer a hint as to the nature of the central object. Using K-corrections and colors for old stellar populations from Kinney et al. (1996), the bulge magnitude $I = 15.08$ corresponds to $M_B = -21.2$. This is quite luminous for a spiral bulge, at about $5 \times 10^{10}\ L_\odot$, and hence with a stellar mass in the bulge of about $3 \times 10^{11}\ M_\odot$. For comparison, this is about 10% more luminous than the bulge of the luminous and bulge-dominated spiral M104 (e.g. Häring & Rix 2006), and

roughly a full magnitude more luminous than any of the 86 bulges observed by de Jong 1996 when transformed to our distance scale. Surface photometry of M104 from Jarvis & Freeman (1985) and Wainscoat et al.(1990) shows that the bulge effective radii are comparable, to within uncertainities in the relative distances caused by the Virgocentric velocity field.

The black hole mass - bulge luminosity fit presented for the highest-quality sample of Ferrarese & Merritt (2000) implies a central mass $8 \times 10^8\ M_\odot$ for this luminosity; the fit for their "less certain" sample differs substantially in this range, giving 3×10^9, which they attributed largely to systematics in modelling central masses when the sphere of influence is not well resolved in the dynamical measurements. Indeed, the reconsideration by Häring & Rix suggests a black-hole mass of $5 \times 10^8\ M_\odot$ for such a bulge.

5. An X-ray jet from a spiral galaxy

The strong absorption against the core X-ray source allows us to look for small-scale extended components at low energies (as also works, for example, for Centaurus A; Kraft et al. 2002). In this case, the core is so faint at low energies that the ACIS data reveal a jet on even smaller angular scales than those recently observed in numerous quasars. As shown in Fig. 8, the structure of 0313-192 changes with energy in a striking way. At the softest energies, we see a jet about $3''$ (4 kpc) long, matching the kpc-scale radio jet mapped by Ledlow et al. (2001). Including photons up to about 1.5 keV, the jet is surrounded by a more extensive sructure which remains too one-sided to attribute to the core PSF. At the highest energies, the structure is completely dominated by the core.

This X-ray jet matches the inner radio jet as well as our resolution and limited photon statistics can show (Fig. 9). We derive an approximate flux from 0.5-3 keV by using an absorbed power-law spectrum of index $\Gamma = 1$. The jet flux is $\approx 8.5 \times 10^{-15}$ erg cm^{-2} s^{-1}, corresponding to a luminosity of 9.3×10^{40} erg s^{-1} in the same band.

This jet is comparable to the jet in M87 in its X-ray properties, as well as the limited photon statistics will let us say. The jet of M87, excluding nuclear emission, has a nearly identical luminosity: about 9×10^{40} erg s^{-1} in the same 0.5-3 keV band, using the knot fluxes from Marshall et al. (2002) and Perlman & Wilson (2005). We averaged the two sets of data; more detailed treatment is unwarranted given that the X-ray flux is variable due (at least) to an occasionally very bright inner knot (i.e. Harris et al. 2006). The radio flux from this part of the jet implies a luminosity rather fainter than in M87, by about a factor 3 (using the 20-cm flux data from Sparks et al. 1996).

This inner jet is measured to be one-sided on kiloparsec scales, with the ratio of southern

to northern jet fluxes greater than about 3 for the soft X-ray band (Fig. 9) and greater than 4 from the radio data of Ledlow et al. (2002). This does not challenge the apparent alignment of the large-scale radio structure with the poles of the spiral disk, since the effects of relativistic beaming are significant even close to the plane of the sky. For a typical spectral index $\alpha = -0.7$ and using the standard equation for jet-counterjet ratio R,

$$R = \left(\frac{1 + \beta \cos\theta}{1 - \beta \cos\theta} \right)^{2-\alpha} \quad (1),$$

$R > 4$ and $\beta \approx 1$ allow any value of the angle between jets and plane of the sky $\theta > 15°$, comparable to the projected angle between jets and poles of the galaxy disk. The observed jet asymmetry is therefore consistent with the notion that the jets emerge within 30° of the polar direction, encountering minimal interstellar gas along the way.

6. Conclusions: Radio source production in a spiral host

These results argue convincingly that 0313-192 is in fact a spiral galaxy (albeit one which we see at a challenging orientation for morphological classification). This prompts us to consider what factors might allow such a demonstrably rare occurrence – not only a kpc-scale radio jet, but an extensive and powerful FR I double radio source – beginning with the salient galaxy properties.

The host galaxy of the radio source 0313-192 is a large, bright spiral, roughly Hubble type Sb. It has a luminous bulge, slightly more luminous than that of M104. The extensive disk is twice as bright as the bulge in the optical, and we can trace luminous H II regions out to at least 17 kpc from the nucleus. The dust lane is thick, richly structured including features reaching several kpc from the midplane, and is seen to nearly 20 kpc from the core. The dust lane shows a warp of several degrees with respect to the stellar disk.

We see the nucleus through an amount of foreground material typical of edge-on, gas-rich spiral disks, as seen both from soft X-ray and 21-cm H I absorption. Likewise, the nucleus is completely obscured in the optical, shortward of about 1.6 μm. The emission lines seen in optical spectroscopy arise mostly in a roughly linear structure seen emerging behind the dust lane on both sides at an angle of about 20°; this structure is seen nearly perpendicular to the radio jets.

If a tidal interaction has taken place, as might be suggested by the disk warp and more strongly inclined inner ionized-gas features, it must have been at large mass ratio (such as acquisition of a gas-rich former companion). The only potential companions close to 0313-192 are dwarf systems. The apparently rich environment, in projection, is part of Abell 428; this

catalogued cluster shows such a large velocity dispersion that it may be largely a large-scale filament seen end-on rather than a traditional galaxy cluster. The redshift data presented by Ledlow et al. (2001) indicate that this filament is broken up into a number of small groups, which could well have associated intragroup hot gas. The environment is important, since production of large-scale radio sources is fostered by interaction with an external medium. However, there is no specific evidence that the external gaseous environment around 0313-192 is unusually dense for a spiral, since a large fraction of spirals are found in groups.

We can picture several circumstances which may contribute to the rarity of extensive double sources in spiral galaxies, and to the ability of 0313-192 to produce such a source. The galaxy is large and luminous, with a bulge luminosity suggesting a central black-hole mass of order $8 \times 10^8\ M_\odot$. This fits with statistical evidence that radio-loud active nuclei have an occurrence which is a strong function of the host galaxy's stellar mass (Best et al. 2005). Furthermore, the jet axis is projected roughly along the minor axis of the galaxy (at an angle of 22°). A polar orientation would make jets more likely to escape the dense interstellar medium of a spiral rather than having their energy dumped into the ISM in a disordered way. Nearby Seyfert galaxies furnish several examples of jets on small scales which lose their collimation rather quickly through interaction with the interstellar medium. In Mkn 78, two small-scale jets are deflected or decollimated during encounters which produce emission-line features (Whittle & Wilson 2004). The anomalous "radio arms" of NGC 4258 are well described as stalled, precessing jets, whose interactions with disk gas can be observed in some detail (Cecil et al. 2000), providing a striking example of how a normal galaxy's interstellar medium can dictate the fate of jets as they propagate from the nucleus. Since the black-hole masses inferred for most Seyferts lie below the mass we suggest from the bulge properties of 0313-192, its jets may well emerge with a higher velocity than the "weak, slow, and heavy" jets (Whittle et al. 2004) seen in many Seyferts.

A requirement for the formation of extensive radio lobes is the escape of jets to eventually encounter an intergalactic medium, which would occur only if they avoided encountering high column densities of cool interstellar gas, possible at high angles to the plane in those spirals with bulges and nuclei that are relatively free from such gas (a condition which probably excludes the many Seyfert galaxies with surrounding star-forming regions, for example).

Aside from 0313-192, the best-attested *disk* galaxy hosting luminous radio jets and lobes is the S0 galaxy NGC 612 (Véron-Cetty & Véron 2001). Their analysis confirmed that it is a bulge-dominated S0 system with stellar disk and dust annulus, confirming the photographic results of Ekers et al. (1978). From their photometric decomposition, the bulge-to-disk ratio in NGC 612 is 2.2 in the i band, much smaller than the value of 0.4 we find from modelling the images of 0313-192. In this comparison, the bulge in NGC 612 remains over twice as

luminous as we find for 0313-192.

Our original interest in studying 0313-192 was to understand the circumstances which allow a spiral galaxy to produce a large double radio source with attendant jets. This detailed analysis leads us to several clues. The galaxy is large and luminous, with a particularly luminous bulge. This in turn suggests that the central black hole is unusually massive for a spiral, so that jets might emerge from its vicinity faster than found in many Seyfert galaxies. The jets emerge roughly along the poles of the disk; if this is needed for them to escape, a further geometric factor limits the number of spirals which could host such radio sources even during episodes of accretion of the black hole. A final contributing factor in this case may be a recent minor merger or weak tidal encounter, which would account for the warped disk and perhaps for more strongly inclined gaseous structure which we see within a few kpc of the nucleus.

This work was supported by NASA through STScI grant HST-GO-09376.01-A, and through Chandra Award Number GO4-5118X issued by the Chandra X-ray Observatory Center, which is operated by the Smithsonian Astrophysical Observatory for and on behalf of the National Aeronautics Space Administration under contract NAS8-03060. This research has made use of the USNOFS Image and Catalogue Archive operated by the United States Naval Observatory, Flagstaff Station (http://www.nofs.navy.mil/data/fchpix/). Fig. 1 attests to the Photoshop wizardry of Zolt Levay. Chris Howk kindly provided a set of WIYN images of edgewise spirals, of which NGC 4565 appears in Fig. 6. The NGC 891 image was taken, in collaboration with Gene Byrd, using the Nordic Optical Telescope, which is operated on the island of La Palma jointly by Denmark, Finland, Iceland, Norway, and Sweden, in the Spanish Observatorio del Roque de los Muchachos of the Instituto de Astrofisica de Canarias. We thank Gijs Verdoes Kleijn for interesting exchanges on how disk galaxies might host strong radio jets, and Lisa Frattare for pointing us to the NGC 5866 Hubble Heritage imagery.

REFERENCES

Antonucci, R. 1993, ARA&A, 31, 473

Arp, H. 1975, PASP, 87, 545

Baganoff, F. K., et al. 2003, ApJ, 591, 891

Bertin, G., & Mark, J. W.-K. 1980, A&A, 88, 289

Best, P. N., Kauffmann, G., Heckman, T. M., Brinchmann, J., Charlot, S., Ivezić, Ž., & White, S. D. M. 2005, MNRAS, 362, 25

Buta, R.J., Corwin, H.G., & Odewahn, S.C. 2006, de Vaucouleurs Atlas of Galaxies (Cambridge, UK: Cambridge University Press), in press

Cecil, G., et al. 2000, ApJ, 536, 675

Clarke, C. J., Kinney, A. L., & Pringle, J. E. 1998, ApJ, 495, 189

Curtis, H. D. 1918, Publ. Lick. Obs.; Vol. 13; Page 45-54, 13, 45

de Grijs, R., Peletier, R. F., & van der Kruit, P. C. 1997, A&A, 327, 966

de Jong, R. S. 1996, A&A, 313, 45

Ekers, R. D., Goss, W. M., Kotanyi, C. G., & Skellern, D. J. 1978, A&A, 69, L21

Evans, D. A., Worrall, D. M., Hardcastle, M. J., Kraft, R. P., & Birkinshaw, M. 2006, ApJ, 642, 96

Ferrarese, L., & Merritt, D. 2000, ApJ, 539, L9

Floyd, D. J. E., Perlman, E., Leahy, J. P., Beswick, R. J., Jackson, N. J., Sparks, W. B., Axon, D. J., & O'Dea, C. P. 2006, ApJ, 639, 23

Fukugita, M., Shimasaku, K., & Ichikawa, T. 1995, PASP, 107, 945

Gallimore, J. F., Baum, S. A., O'Dea, C. P., Pedlar, A., & Brinks, E. 1999, ApJ, 524, 684

Grandi, P., Malaguti, G., & Fiocchi, M. 2006, ApJ, 642, 113

Häring, N., & Rix, H.-W. 2004, ApJ, 604, L89

Harris, D. E., Cheung, C. C., Biretta, J. A., Sparks, W. B., Junor, W., Perlman, E. S., & Wilson, A. S. 2006, ApJ, 640, 211

Heckman, T. M., & Balick, B. 1979, A&A, 76, L7

Heckman, T. M., Miley, G. K., Balick, B., van Breugel, W. J. M., & Butcher, H. R. 1982, ApJ, 262, 529

Heckman, T. M., Smith, E. P., Baum, S. A., van Breugel, W. J. M., Miley, G. K., Illingworth, G. D., Bothun, G. D., & Balick, B. 1986, ApJ, 311, 526

Howk, J. C., & Savage, B. D. 1999, AJ, 117, 2077

Hunter, C., & Toomre, A. 1969, ApJ, 155, 747

Jackson, N., Beswick, R., Pedlar, A., Cole, G. H., Sparks, W. B., Leahy, J. P., Axon, D. J., & Holloway, A. J. 2003, MNRAS, 338, 643

Jarvis, B. J., & Freeman, K. C. 1985, ApJ, 295, 324

Kinney, A. L., Calzetti, D., Bohlin, R. C., McQuade, K., Storchi-Bergmann, T., & Schmitt, H. R. 1996, ApJ, 467, 38

Koopmann, R. A., & Kenney, J. D. P. 2006, ApJS, 162, 97

Kraft, R. P., Forman, W. R., Jones, C., Murray, S. S., Hardcastle, M. J., & Worrall, D. M. 2002, ApJ, 569, 54

Ledlow, M. J., Owen, F. N., & Keel, W. C. 1998, ApJ, 495, 227

Ledlow, M. J., Owen, F. N., Yun, M. S., & Hill, J. M. 2001, ApJ, 552, 120

Macchetto, F., Pastoriza, M., Caon, N., Sparks, W. B., Giavalisco, M., Bender, R., & Capaccioli, M. 1996, A&AS, 120, 463

Marshall, H. L., Miller, B. P., Davis, D. S., Perlman, E. S., Wise, M., Canizares, C. R., & Harris, D. E. 2002, ApJ, 564, 683

Matthews, T. A., Morgan, W. W., & Schmidt, M. 1964, ApJ, 140, 35

Percival, W. J., Miller, L., McLure, R. J., & Dunlop, J. S. 2001, MNRAS, 322, 843

Perlman, E. S., & Wilson, A. S. 2005, ApJ, 627, 140

Pogge, R. W., & Eskridge, P. B. 1993, AJ, 106, 1405

Pohlen, M., Dettmar, R.-J., Lütticke, R., & Schwarzkopf, U. 2000, A&AS, 144, 405

Ptak, A., Zakamska, N. L., Strauss, M. A., Krolik, J. H., Heckman, T. M., Schneider, D. P., & Brinkmann, J. 2006, ApJ, 637, 147

Roche, N., & Eales, S. A. 2000, MNRAS, 317, 120

Sandage, A., & Bedke, J. 1994, Carnegie Atlas of Galaxies (Washington, DC: Carnegie Institution of Washington with The Flintridge Foundation)

Sandage, A., & Tammann, G. A. 1981, Washington: Carnegie Institution, 1981

Sandage, A., & Tammann, G. A. 1987, Carnegie Institution of Washington Publication, Washington: Carnegie Institution, 1987, 2nd ed.

Schwarzkopf, U., & Dettmar, R.-J. 1997, Astronomische Gesellschaft Meeting Abstracts, 13, 238

Sparks, W. B., Biretta, J. A., & Macchetto, F. 1996, ApJ, 473, 254

Steenbrugge, K. C., Kaastra, J. S., Sako, M., Branduardi-Raymont, G., Behar, E., Paerels, F. B. S., Blustin, A. J., & Kahn, S. M. 2005, A&A, 432, 453

van Breugel, W., Heckman, T., Butcher, H., & Miley, G. 1984, ApJ, 277, 82

van der Kruit, P. C., & Searle, L. 1981, A&A, 95, 116

Véron-Cetty, M. P., & Véron, P. 2001, A&A, 375, 791

Wainscoat, R. J., Hyland, A. R., & Freeman, K. C. 1990, ApJ, 348, 85

Whittle, M., Silverman, J. D., Rosario, D. J., Wilson, A. S., & Nelson, C. H. 2004, IAU Symposium, 222, 299

Whittle, M., & Wilson, A. S. 2004, AJ, 127, 606

Fig. 1.— The radio galaxy 0313-192 and its environment, in a color composite produced from the ACS images in F555W and F814W. The red overlay shows VLA 20-cm structure, encompassing a wide field of 82×96 arcseconds to show most of the radio source. Multiple arrays have been combined to retain higher resolution in the kpc-scale jet. This image is available as STScI-PRC03-04. North is about 20° counterclockwise from the top. The less inclined spiral has a substantially different redshift and, while likely part of Abell 428, does not form a bound interacting system with 0313-192.

Fig. 2.— The radio galaxy 0313-192, in a color composite produced from the ACS images in F555W and F814W. The radio galaxy is shown here with an offset logarithmic intensity scale to compress the image's dynamic range. North is 5° degrees clockwise from the top. This display, covering 20.0×28.3 arcseconds, emphasizes the complex absorption structure of the disk dust. In the color scheme, blue corresponds to the F555W (V) image, red to F775W (I), and green to their mean.

Fig. 3.— Hα and [O III] images with the narrowband ramp filters, after continuum subtraction. Color gradients leave negative residuals in parts of the dust lane. Each image has been rotated by 23.4° to align with the mean starlight plane, and spans 14.2×22.0 arcseconds. North-northwest is at the top.

Fig. 4.— JHK images of 0313-192. from FLAMINGOS on *Gemini-S*. Each panel spans 9.5×32.3 arcseconds and is shown with north at the top.

Fig. 5.— Photometric profiles, in the F814W I band, of the edge-on stellar disk in 0313-192. The best-fit de Vaucouleurs bulge model was subtracted before producing these profiles. The top panel shows profiles parallel to the disk plane, averaged over regions from 0.8-1.6" north and south of the mean midplane. The curve shows the projection of a truncated exponential disk, as is seen in nearby edge-on spirals. The lower panel illustrates the "vertical" profile normal to the disk plane, which is well modelled (away from the dust lane) by an exponential, again as seen for local edge-on spirals.

Fig. 6.— Comparison of dust structures in 0313-192, from the ACS V image (center), with nearby objects having well-defined Hubble types. Each is shown on an intensity scale which is logarithmic after a small offset (1% of peak) to reduce the appearance of sky noise. The filaments of dust perpendicular to the plane are shared among all the spirals, and 0313-192 shows well-developed perpendicular structures of this kind. Radial truncation of the dust disk relative to the stellar disk is characteristic of S0 systems, as exhibited only by NGC 5866 at the top. The NGC 4565 image is from Howk & Savage (1999); NGC 891 was observed with the Nordic Optical Telescope, and the remaining comparison images are taken from the HST archive.

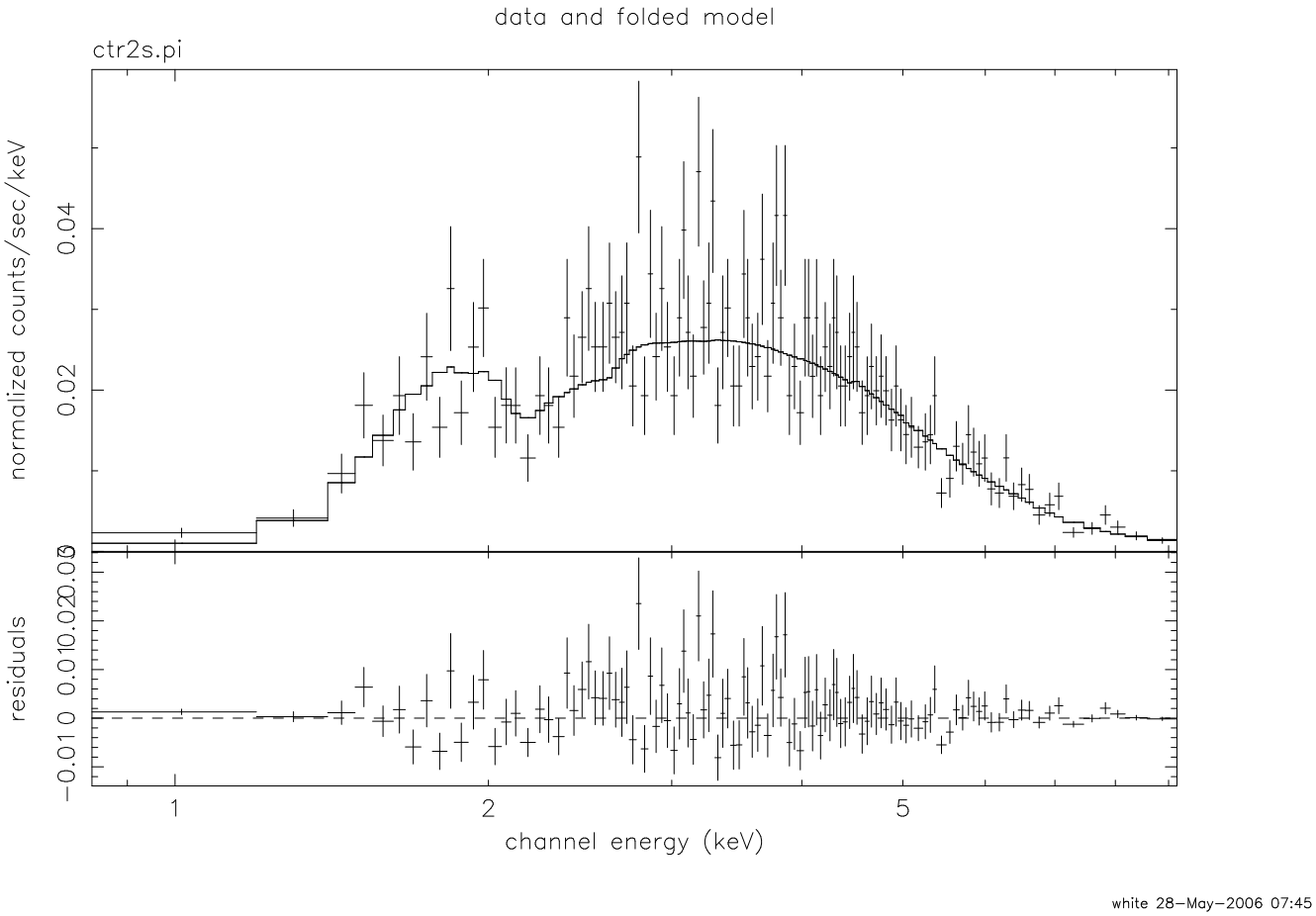

Fig. 7.— *Chandra* ACIS spectrum of photons within 2″of the peak of 0313-192, and the best-fit absorbed power-law fit. Properties of this fit are: photon index $\Gamma = 1.33^{+0.34}_{-0.27}$ and an intrinsic absorbing column of $N_H = 4.06^{+0.73}_{-0.58} \times 10^{22}$ cm^{-2} (90% confidence intervals). The lower panel shows residuals from this fit.

Fig. 8.— *Chandra* ACIS images of the core region of 0313-192 in various energy bands. At low energies, the strong absorption against the core allows a small-scale X-ray jet to be seen (left). At intermediate energies, we see a broader asymmetric halo of X-ray structure, while the core source dominates at the highest energied measured (right). Each image was produced by mapping the event list on a 0.125-″grid, then convolving with a Gaussian of 0.75″FWHM.

Fig. 9.— *Chandra* ACIS image of the jet in 0313-192, using events from 0.35-1.2 keV and a smoothing of 1″FWHM, compared to the 8.4 GHz structure as measured using the VLA (Ledlow et al. 2001). The low-energy X-ray structure traces the radio jet.

This figure "f1.jpg" is available in "jpg" format from:

http://arXiv.org/ps/astro-ph/0608086

This figure "f2.jpg" is available in "jpg" format from:

http://arXiv.org/ps/astro-ph/0608086

This figure "f3.jpg" is available in "jpg" format from:

http://arXiv.org/ps/astro-ph/0608086

This figure "f4.jpg" is available in "jpg" format from:

http://arXiv.org/ps/astro-ph/0608086

This figure "f5.gif" is available in "gif" format from:

http://arXiv.org/ps/astro-ph/0608086

This figure "f6.jpg" is available in "jpg" format from:

http://arXiv.org/ps/astro-ph/0608086

This figure "f8.jpg" is available in "jpg" format from:

http://arXiv.org/ps/astro-ph/0608086

This figure "f9.jpg" is available in "jpg" format from:

http://arXiv.org/ps/astro-ph/0608086